Structure of the $^6Li \rightarrow p + (n\alpha)$ vertex: Three-body formalism

C. T. Christou,* D. R. Lehman, and W. C. Parke
Department of Physics, The George Washington University, Washington, D.C. 20052
(Received 20 August 1987)

Three-body models of ^6Li are used to investigate the structure of the $^6Li \rightarrow p + (n\alpha)$ vertex amplitude. Within the three-body framework, the formalism of the $^6Li \rightarrow p + (n\alpha)$ overlap amplitude is delineated. From this overlap, the formula for the central physical quantity, namely, the $^6Li \rightarrow p + (n\alpha)$ joint momentum distribution, is derived. It is shown that the $^6Li \rightarrow p + (n\alpha)$ joint momentum distribution satisfies a sum rule consistent with its probability interpretation. The sum rule is used as a check on the numerical calculation of the joint momentum distribution and to isolate terms that contribute insignificantly. By integration of the $^6Li \rightarrow p + (n\alpha)$ joint momentum distribution over a given range of the $n\alpha$ excitation energy, the momentum distribution of the valence proton in ^6Li is obtained. From both the $^6Li \rightarrow p + (n\alpha)$ joint momentum distribution and the p-$(n\alpha)$ momentum distribution, the dynamical structure of the $^6Li \rightarrow p + (n\alpha)$ vertex according to three-body models is uncovered.

I. INTRODUCTION

From the viewpoint of an alpha-particle (α) plus two-nucleon (NN) three-body model of ^6Li, there are three possible virtual-disintegration amplitudes for ^6Li: (1) $^6Li \rightarrow \alpha + d$, where d means deuteron; (2) $^6Li \rightarrow \alpha + (np)$, where the parentheses around the np indicate that the neutron (n) and proton (p) are interacting in an unbound state; and (3) $^6Li \rightarrow p + (n\alpha)$ or $^6Li \rightarrow n + (p\alpha)$, both equivalent in this work since we neglect the Coulomb interaction. The $^6Li \rightarrow \alpha + d$ case has been treated in earlier work[1] and the predictions for the $^6Li \rightarrow \alpha + d$ momentum distribution have recently been tested against data obtained from the $^6Li(e,e'd)\alpha$ reaction.[2] It is found that three-body models describe well the $^6Li \rightarrow \alpha + d$ vertex for α-d relative momenta up to ~ 300 MeV/c. In fact, the predicted $2s$ character of the α-d relative wave function is clearly illustrated by the data.[2] On the other hand, no work has been done on the $^6Li \rightarrow \alpha + (np)$ and $^6Li \rightarrow p + (n\alpha)$ vertices from the viewpoint of ^6Li three-body models. For the $^6Li \rightarrow \alpha + (np)$ case, this is mainly due to the absence of experimental data to compare with predictions. As a consequence, this amplitude will be considered at a future time in conjunction with pending $^6Li(e,e'\alpha)np$ experiments.[3] However, measurements have existed for a long time that were aimed at uncovering the physics of the $^6Li \rightarrow p + (n\alpha)$ vertex.[4] Data of varying quality, limited in some cases by energy resolution and in others by too low an incident-projectile energy, are available from $^6Li(p,2p)n\alpha$ and $^6Li(e,e'p)n\alpha$ experiments. Moreover, new high-resolution data for $^6Li(e,e'p)n\alpha$, with incident electron energies of 400–500 MeV, will soon become available. Thus, we now apply the theory of ^6Li three-body models to the $^6Li \rightarrow p + (n\alpha)$ vertex.

The general aim of this series of papers is to examine in detail the structure of the $^6Li \rightarrow p + (n\alpha)$ vertex from the framework of three-body models of ^6Li. The present paper gives the formalism for computation of the $^6Li \rightarrow p + (n\alpha)$ vertex amplitude or the overlap amplitude. Once the formalism is established, the probability of finding within ^6Li a proton moving with momentum $\mathbf{q}$ relative to the center of mass of an interacting $n\alpha$ pair, where the $n\alpha$ relative momentum is $\boldsymbol{\kappa}$, per momentum-space volume squared, can be calculated. This "joint" momentum distribution forms the basis for the following two papers, which concern the reactions $^6Li(p,2p)n\alpha$ and $^6Li(e,e'p)n\alpha$, respectively.

The present paper is organized as follows: Section II contains the general formalism for setting up the $^6Li \rightarrow p + (n\alpha)$ vertex amplitude, a review of the form of the ^6Li three-body wave function, and a concise presentation of the $n\alpha$ scattering wave function. In Sec. III the $^6Li \rightarrow p + (n\alpha)$ joint momentum distribution is derived. As a means of checking numerical calculations, it is shown that the joint momentum distribution must satisfy a sum rule based on the normalization of the ^6Li ground-state wave function. Numerical results for various three-body models are given in Sec. IV: the sum rule is checked and the joint momentum distribution obtained. The physics underlying the results for the joint momentum distribution is discussed in Sec. V, followed by a brief conclusion in Sec. VI. An Appendix contains a derivation of the $n\alpha$ scattering-state completeness that leads to the above-mentioned sum rule.

II. VERTEX FORMALISM

The virtual-disintegration amplitude for $^6Li \rightarrow p + (n\alpha)$ is depicted by the Feynman diagram of Fig. 1. The ^6Li nucleus is taken to be at rest. As a consequence, if the relative momentum of the proton with respect to the center of mass (c.m.) of the $n\alpha$ pair is $+\mathbf{q}$, the $n\alpha$-pair c.m. recoils with momentum $-\mathbf{q}$. In addition, the relative momentum of the n and α is designated as $\boldsymbol{\kappa}$. The amplitude will be called $M(\mathbf{q},\boldsymbol{\kappa}; m_p, m_n, m_6)$, where the m_i represent the magnetic quantum numbers of the proton, neutron, and ^6Li nucleus, respectively.

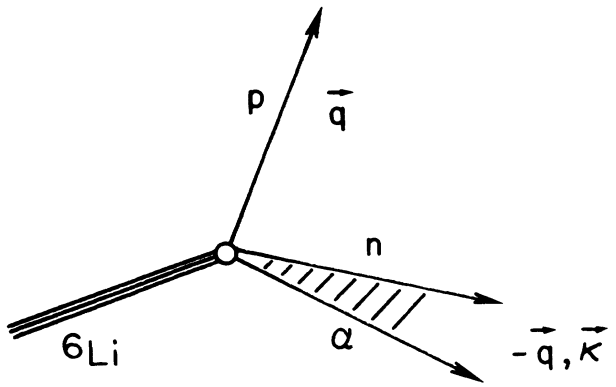

FIG. 1. Feynman diagram for the virtual-disintegration process $^6\mathrm{Li}\rightarrow \mathrm{p}+(\mathrm{n}\alpha)$.

The virtual-disintegration amplitude is defined as follows:

$$M(\mathbf{q},\boldsymbol{\kappa};m_{\mathrm{p}},m_{\mathrm{n}},m_6)\equiv\langle \mathbf{q}\chi^{[1/2]}_{m_{\mathrm{p}}}\varphi^{(-)}_{\kappa,m_{\mathrm{n}}} \mid V_{\mathrm{np}}+V_{\mathrm{p}\alpha} \mid \Psi^{[1]}_{m_6}\rangle \ , \tag{1}$$

where $\chi^{[1/2]}_{m_{\mathrm{p}}}$ is the spin-$\frac{1}{2}$ spinor for the proton, $\varphi^{(-)}_{\kappa,m_{\mathrm{n}}}$ is the outgoing scattering state (incoming wave) for the nα pair, the potentials are the excluded interactions in the final state, and $\Psi^{[1]}_{m_6}$ represents the ^{6}Li ground state. Since the ^{6}Li ground state, thought of as a three-body nucleus, satisfies Schrödinger's equation in the form

$$(H_0+V_{\mathrm{np}}+V_{\mathrm{p}\alpha}+V_{\mathrm{n}\alpha})\mid\Psi^{[1]}_{m_6}\rangle=-B_6\mid\Psi^{[1]}_{m_6}\rangle \ , \tag{2}$$

where H_0 is the three-body (αnp) kinetic-energy operator and B_6 is the binding energy, we can write Eq. (1) as

$$M(\mathbf{q},\boldsymbol{\kappa};m_{\mathrm{p}},m_{\mathrm{n}},m_6)=-\left[\frac{3q^2}{5M}+\frac{5\kappa^2}{8M}+B_6\right]\times\langle \mathbf{q}\chi^{[1/2]}_{m_{\mathrm{p}}}\varphi^{(-)}_{\kappa,m_{\mathrm{n}}}\mid\Psi^{[1]}_{m_6}\rangle \ , \tag{3}$$

which follows from

$$\langle \mathbf{q}\chi^{[1/2]}_{m_{\mathrm{p}}}\varphi^{(-)}_{\kappa,m_{\mathrm{n}}}\mid(H_0+V_{\mathrm{n}\alpha})=\langle \mathbf{q}\chi^{[1/2]}_{m_{\mathrm{p}}}\varphi^{(-)}_{\kappa,m_{\mathrm{n}}}\mid\left[\frac{3q^2}{5M}+\frac{5\kappa^2}{8M}\right] \ . \tag{4}$$

Thus, the key element in calculating the virtual-disintegration amplitude $M(\mathbf{q},\boldsymbol{\kappa};m_{\mathrm{p}},m_{\mathrm{n}},m_6)$ is the $^6\mathrm{Li}\rightarrow\mathrm{p}+(\mathrm{n}\alpha)$ overlap amplitude, hereafter denoted

$$A(\mathbf{q},\boldsymbol{\kappa};m_{\mathrm{p}},m_{\mathrm{n}},m_6)=\langle \mathbf{q}\chi^{[1/2]}_{m_{\mathrm{p}}}\varphi^{(-)}_{\kappa,m_{\mathrm{n}}}\mid\Psi^{[1]}_{m_6}\rangle \ . \tag{5}$$

All calculations described in this series of papers are carried out in momentum space. The explicit expression of $A(\mathbf{q},\ldots)$ in terms of wave functions in momentum representation is

$$A(\mathbf{q},\boldsymbol{\kappa};m_{\mathrm{p}},m_{\mathrm{n}},m_6)=\int d^3p\,d^3k\,\langle \mathbf{q}\chi^{[1/2]}_{m_{\mathrm{p}}}\varphi^{[1/2]^{(-)}}_{\kappa,m_{\mathrm{n}}}\mid\mathbf{pk}\rangle\cdot\langle\mathbf{pk}\mid\Psi^{[1]}_{m_6}\rangle \tag{6}$$

$$=\int d^3p\,d^3k\,\Phi^{[1/2]\dagger}_{\mathbf{q},m_{\mathrm{p}}}(\mathbf{p})\varphi^{[1/2]^{(-)\dagger}}_{\kappa,m_{\mathrm{n}}}(\mathbf{k})\Psi^{[1]}_{m_6}(\mathbf{p},\mathbf{k}) \ , \tag{7}$$

where $\mathbf{p}$ and $\mathbf{k}$ are Jacobi momenta appropriate to the p-(nα) permutation. Specifically,

$$\Phi^{[1/2]}_{\mathbf{q},m_{\mathrm{p}}}(\mathbf{p})=\delta^3(\mathbf{p}-\mathbf{q})\chi^{[1/2]}_{m_{\mathrm{p}}} \ , \tag{8}$$

whereas the nα-scattering state is given by

$$\varphi^{[1/2]^{(-)}}_{\kappa,m_{\mathrm{n}}}(\mathbf{k})=\left[\delta^3(\mathbf{k}-\boldsymbol{\kappa})+\frac{1}{2\pi^2}\frac{1}{k^2-\kappa^2+i\eta}\sum_{J=1/2}^{3/2}\sum_{\substack{\ell=J-1/2\\ \ell\le 1}}^{J+1/2}(-1)^{2J}\hat{J}\frac{h^J_\ell(k)}{h^J_\ell(\kappa)}f^{J(-)}_\ell(\kappa)4\pi[\mathcal{Y}^{[J]}_{\ell\,1/2}(\hat{\mathbf{k}})\times\tilde{\mathcal{Y}}^{[J]}_{\ell\,1/2}(\hat{\boldsymbol{\kappa}})]^{[0]}\right]\chi^{[1/2]}_{m_{\mathrm{n}}} \ , \tag{9}$$

where the partial-wave scattering amplitudes are defined by

$$f^{J(-)}_\ell(\kappa)=\frac{2\pi^2\Lambda^J_\ell(h^J_\ell(\kappa))^2}{1-\Lambda^J_\ell I^{J(-)}_\ell(\kappa)} \ , \tag{10}$$

with

$$I^{J(-)}_\ell(\kappa)=\int d^3k\frac{[h^J_\ell(k)]^2}{k^2-\kappa^2+i\eta} \ . \tag{11}$$

Equation (9) follows from the interactions used in earlier work to generate the ^{6}Li ground-state wave function:[5] the nα pair interacts in the dominant partial-wave states at low energies, i.e., the $S_{1/2}$, $P_{1/2}$, and $P_{3/2}$, and the interactions are assumed to be represented by separable potentials. All notation follows that of Ref. 5, e.g., Λ^J_ℓ is the strength of the partial wave ℓ, total angular momentum, J, interaction, and $h^J_\ell(k)$ is the corresponding interaction form factor. Of course, an important aspect of this work is the fact that the initial and final states originate from the same underlying two-body interactions.

From Eq. (7), our objective is to derive an expression for the overlap amplitude that yields easily to numerical computation. There are two main terms in Eq. (7): (1) The pure plane-wave term, and (2) The term with the nα scattering amplitudes. This leads us to break the overlap amplitude into a sum of two pieces denoted by subscripts p (plane wave) and s (scattering). By means of partial-wave expansion of the Dirac delta functions and recoupling of the angular functions with the spin functions, we can write

$$\delta^3(\mathbf{p}-\mathbf{q})\delta^3(\mathbf{k}-\boldsymbol{\kappa})\chi^{[1/2]}_{m_p}\chi^{[1/2]}_{m_n}=\frac{\delta(p-q)}{p^2}\frac{\delta(k-\kappa)}{k^2}\sum_{\substack{K\\LL'\\\mathcal{L}\mathcal{J}\\GG'}}\langle\tfrac{1}{2}m_p\,\tfrac{1}{2}m_n\,|\,K\,M\rangle(-1)^{\mathcal{J}+\mathcal{L}+K}\hat{\mathcal{J}}\hat{\mathcal{L}}\hat{G}\hat{G}'\begin{Bmatrix}L & L' & \mathcal{L}\\ \frac{1}{2} & \frac{1}{2} & K\\ G & G' & \mathcal{J}\end{Bmatrix}$$

$$\times[[Y^{[L]}(\hat{\mathbf{q}})\times Y^{[L']}(\hat{\boldsymbol{\kappa}})]^{[\mathcal{L}]}\times[\mathcal{Y}^{[G]}_{L\,1/2}(\hat{\mathbf{p}},1)\times\mathcal{Y}^{[G']}_{L'\,1/2}(\hat{\mathbf{k}},2)]^{[\mathcal{J}]}]^{[K]}_{M}\,, \tag{12}$$

where

$$\mathcal{Y}^{[G]}_{L\,1/2}(\hat{\mathbf{p}},1)=\sum_{\eta\mu}\langle L\,\eta\,\tfrac{1}{2}\mu\,|\,G\,m_G\rangle Y^{[L]}_{\eta}(\hat{\mathbf{p}})\chi^{[1/2]}_{\mu}(1)\,, \tag{13}$$

the proton is denoted particle 1 and the neutron particle 2, and the angular-momentum notation follows Ref. 5. When Eq. (12) is substituted into Eq. (7), the plane-wave part of the overlap amplitude becomes

$$A_p(\mathbf{q},\boldsymbol{\kappa};m_p,m_n,m_6)=\sum_{\substack{K\\LL'\\\mathcal{L}M_{\mathcal{L}}\\GG'}}\langle\tfrac{1}{2}m_p\,\tfrac{1}{2}m_n\,|\,K\,M\rangle(-1)^{1+\mathcal{L}+K}$$

$$\times\hat{\mathcal{L}}\hat{G}\hat{G}'\begin{Bmatrix}L & L' & \mathcal{L}\\ \frac{1}{2} & \frac{1}{2} & K\\ G & G' & 1\end{Bmatrix}\langle\mathcal{L}M_{\mathcal{L}}\,1\,m_6\,|\,K\,M\rangle[Y^{[L]}(\hat{\mathbf{q}})\times Y^{[L']}(\hat{\boldsymbol{\kappa}})]^{[\mathcal{L}]\dagger}_{M_{\mathcal{L}}}$$

$$\times\int_0^\infty dp\,\delta(p-q)\int_0^\infty dk\,\delta(k-\kappa)\int d\Omega_p d\Omega_k[[\tilde{\mathcal{Y}}^{[G]}_{L\,1/2}(\hat{\mathbf{p}},1)\times\tilde{\mathcal{Y}}^{[G']}_{L'\,1/2}(\hat{\mathbf{k}},2)]^{[1]}\times\Psi^{[1]}(\mathbf{p},\mathbf{k})]^{[0]}\,. \tag{14}$$

A similar procedure can be used on the the term that accounts for the nα scattering. In detail, the first step is to consider

$$\delta^3(\mathbf{p}-\mathbf{q})\chi^{[1/2]}_{m_p}[\mathcal{Y}^{[J]}_{\ell\,1/2}(\hat{\mathbf{k}})\times\tilde{\mathcal{Y}}^{[J]}_{\ell\,1/2}(\hat{\boldsymbol{\kappa}})]^{[0]}\chi^{[1/2]}_{m_n}$$

$$=\frac{\delta(p-q)}{p^2}\sum_{\substack{KL\\\mathcal{L}\mathcal{J}\\G}}\langle\tfrac{1}{2}m_p\,\tfrac{1}{2}m_n\,|\,K\,M\rangle(-1)^{\mathcal{J}+\mathcal{L}+K+1}$$

$$\times\hat{\mathcal{J}}\hat{\mathcal{L}}\hat{G}\begin{Bmatrix}L & \ell & \mathcal{L}\\ \frac{1}{2} & \frac{1}{2} & K\\ G & J & \mathcal{J}\end{Bmatrix}[[Y^{[L]}(\hat{\mathbf{q}})\times Y^{[\ell]}(\hat{\boldsymbol{\kappa}})]^{[\mathcal{L}]}\times[\mathcal{Y}^{[G]}_{L\,\frac{1}{2}}(\hat{\mathbf{p}},1)\mathcal{Y}^{[J]}_{\ell\,1/2}(\hat{\mathbf{k}},2)]^{[\mathcal{J}]}]^{[K]}_{M}\,. \tag{15}$$

Making use of Eq. (15) in Eq. (7), we derive for the scattering part of the overlap amplitude the following:

$$A_s(\mathbf{q},\boldsymbol{\kappa};m_p,m_n,m_6)=\sum_{J\ell}\sum_{\substack{KL\\\mathcal{L}M_{\mathcal{L}}\\G}}\langle\tfrac{1}{2}m_p\,\tfrac{1}{2}m_n\,|\,K\,M\rangle(-1)^{1+\mathcal{L}+K}$$

$$\times\hat{\mathcal{L}}\hat{G}\hat{J}\begin{Bmatrix}L & \ell & \mathcal{L}\\ \frac{1}{2} & \frac{1}{2} & K\\ G & J & \mathcal{J}\end{Bmatrix}\langle\mathcal{L}M_{\mathcal{L}}\,1\,m_6\,|\,K\,M\rangle[Y^{[L]}(\hat{\mathbf{q}})\times Y^{[l]}(\hat{\boldsymbol{\kappa}})]^{[\mathcal{L}]\dagger}_{M_{\mathcal{L}}}$$

$$\times\frac{2}{\pi}\frac{f^{J(-)\dagger}_{\ell}(\kappa)}{h^{J}_{\ell}(\kappa)}\int_0^\infty dp\,\delta(p-q)\int_0^\infty k^2dk\frac{h^{J}_{\ell}(k)}{k^2-\kappa^2-i\eta}$$

$$\times\int d\Omega_p d\Omega_k[[\tilde{\mathcal{Y}}^{[G]}_{L\,1/2}(\hat{\mathbf{p}},1)\times\tilde{\mathcal{Y}}^{[J]}_{\ell\,1/2}(\hat{\mathbf{k}},2)]^{[1]}$$

$$\times\Psi^{[1]}(\mathbf{p},\mathbf{k})]^{[0]}\,. \tag{16}$$

The final element that is needed in the derivation of the overlap amplitude is the ground-state wave function. Following Ref. 5, we write

$$\Psi^{[1]}_{m_6}(\mathbf{p}_3,\mathbf{k}_{12})=\frac{4\pi N}{\bar{K}^2+k_{12}^2+\frac{3}{8}p_3^2}\left[\lambda_1\sum_{\substack{\ell,\ell'=0\\(\neq 1)}}^{2} g^1_\ell(k_{12})[[Y^{[\ell]}(\hat{\mathbf{k}}_{12})\times\chi^{[1]}(12)]^{[1]}\times Y^{[\ell']}(\hat{\mathbf{p}}_3)]^{[1]}_{m_6}G^{\ell'}(p_3)\right.$$
$$+\tfrac{5}{8}\sum_{J=1/2}^{3/2}\sum_{J'=|1-J|}^{1+J}\sum_{\substack{\ell=J-1/2\\(\leq 1)}}^{J+1/2}\sum_{\ell'=J'-1/2}^{J'+1/2}P^{\ell+\ell'}\Lambda^J_\ell\{h^J_\ell(k_{23})$$
$$\times[\mathcal{Y}^{[J]}_{\ell\,1/2}(\hat{\mathbf{k}}_{23},2)\times\mathcal{Y}^{[J']}_{\ell'\,1/2}(\hat{\mathbf{p}}_1,1)]^{[1]}_{m_6}$$
$$\left.\times F^{J'}_{\ell'(J\ell)}(p_1)+(-1)^\ell(31,2)\}\right], \qquad (17)$$

where N is the normalization constant, $G^{\ell'}$ and $F^{J'}_{\ell'(J\ell)}$ are the spectator functions, and $\bar{K}^2=MB_6$. A numerically tractable equation for the overlap amplitude is obtained by performing the angular-spin projections on $\Psi^{[1]}_{m_6}$ that are indicated in Eqs. (14) and (16). This is a straightforward, but tedious task. Since the final expressions are lengthy, we do not display them here.

In closing this section, we bring to the reader's attention the general form of the overlap amplitude. Examination of Eqs. (14) and (16) indicates that

$$A(\mathbf{q},\boldsymbol{\kappa};m_{\rm p},m_{\rm n},m_6)=\sum_{\substack{K\\ \mathcal{L}M_{\mathcal{L}}}}\langle\tfrac{1}{2}m_{\rm p}\,\tfrac{1}{2}m_{\rm n}\,|\,K\,M\rangle(-1)^{\mathcal{L}}\hat{\mathcal{L}}\langle\mathcal{L}\,M_{\mathcal{L}}\,1\,m_6\,|\,K\,M\rangle\mathcal{A}^{[\mathcal{L}]}_{M_{\mathcal{L}}}(K;\mathbf{q},\boldsymbol{\kappa}), \qquad (18)$$

where K can be only 0 or 1, and thus $\mathcal{L}=1$ or $0\leq\mathcal{L}\leq 2$, respectively. In the next section, Eq. (18) forms the basis for the derivation of the ^{6}Li$\rightarrow$p + (nα) joint momentum distribution.

III. JOINT MOMENTUM DISTRIBUTION

The quantity of current physical interest with respect to the ^{6}Li$\rightarrow$p + (nα) vertex is the joint momentum distribution: The probability of finding within ^{6}Li a proton moving with momentum q relative to the center of mass of an interacting nα pair that has relative momentum κ per unit momentum volume per unit momentum cubed. In principle, the joint momentum distribution or integrals thereof can be extracted from (p,2p) or (e,e'p) coincidence experiments as discussed in the following two papers, respectively.

The derivation of the joint momentum distribution follows from Eq. (18). In the experiments that we shall consider, the ^{6}Li target is unpolarized and the recoiling nα pair goes undetected. Therefore, we shall average over the ^{6}Li spin and sum over the spin of the neutron. From Eq. (18), we form

$$\tfrac{1}{3}\sum_{m_6}\sum_{m_{\rm n}}A^\dagger(\mathbf{q},\boldsymbol{\kappa};m_{\rm p},m_{\rm n},m_6)A(\mathbf{q},\boldsymbol{\kappa};m'_{\rm p},m_{\rm n},m_6)$$
$$=\frac{(-1)^{m_{\rm p}+1/2}}{3}\sum_{\substack{KK'\\ \mathcal{L}\mathcal{L}'\\ TM_T}}\hat{K}^2\hat{K}'^2\hat{\mathcal{L}}\hat{\mathcal{L}}'(-1)^{\mathcal{L}'}\hat{T}\begin{pmatrix}\frac{1}{2} & T & \frac{1}{2}\\ m_{\rm p} & M_T & -m'_{\rm p}\end{pmatrix}$$
$$\times\begin{Bmatrix}K & K' & T\\ \mathcal{L}' & \mathcal{L} & 1\end{Bmatrix}\begin{Bmatrix}K & K' & T\\ \frac{1}{2} & \frac{1}{2} & \frac{1}{2}\end{Bmatrix}[\bar{\mathcal{A}}^{[\mathcal{L}]}(K;\mathbf{q},\boldsymbol{\kappa})\times\mathcal{A}^{[\mathcal{L}']}(K';\mathbf{q},\boldsymbol{\kappa})]^{[T]}_{M_T}, \qquad (19)$$

where some recoupling algebra has been carried out to obtain the result on the right-hand side of Eq. (19). The bar over $\mathcal{A}^{[\mathcal{L}]}$ means that the complex conjugate is to be taken, both for the scattering amplitude and propagator [see Eq. (16)]. From Eqs. (14) and (16), it is seen that the angular-momentum structure of $\mathcal{A}^{[\mathcal{L}]}$ comes from the coupling of the $\hat{\mathbf{q}}$ and $\hat{\boldsymbol{\kappa}}$ spherical harmonics. Furthermore, as mentioned above, the nα pair goes unobserved in the experiments that we shall consider. Thus, we integrate over the directions of $\hat{\mathbf{q}}$ and $\hat{\boldsymbol{\kappa}}$ in Eq. (19):

$$\frac{1}{4\pi}\int d\Omega_q \int d\Omega_\kappa \frac{1}{3}\sum_{\substack{m_6\\ m_n}} A^\dagger(\mathbf{q},\boldsymbol{\kappa};m_p,m_n,m_6)A(\mathbf{q},\boldsymbol{\kappa};m'_p,m_n,m_6)=\frac{\delta_{m_p m'_p}}{2}V(\kappa,q)\ , \tag{20}$$

where

$$V(\kappa,q)\equiv\frac{1}{3}\sum_{\substack{K\\ \mathcal{L}}}\hat{K}^2\hat{\mathcal{L}}\frac{1}{4\pi}\int d\Omega_q\int d\Omega_\kappa[\overline{\mathcal{A}}^{[\mathcal{L}]}(K;\mathbf{q},\boldsymbol{\kappa})\times\mathcal{A}^{[\mathcal{L}]}(K;\mathbf{q},\boldsymbol{\kappa})]^{[0]} \tag{21}$$

is the joint momentum distribution. [We shall see in the third paper of this series that the ^{6}Li$\rightarrow$p + (nα) spectral function, denoted $S(E_\kappa,q)$, is equal to $\mu_{\alpha n}\kappa V(\kappa,q)$.] Equation (21) is the basis for our calculations.

Owing to the normalization of the ^{6}Li ground-state wave function and the completeness of the plane-wave and scattering states (for the latter, see the Appendix), $V(\kappa,q)$ satisfies a sum rule, i.e.,

$$4\pi\int_0^\infty q^2dq\int_0^\infty\kappa^2d\kappa\,V(\kappa,q)=1\ . \tag{22}$$

To obtain this condition on the joint momentum distribution, we begin from the ground-state normalization condition, i.e.,

$$\frac{1}{3}\sum_{m_6}\langle\Psi^{[1]}_{m_6}\mid\Psi^{[1]}_{m_6}\rangle=1\ . \tag{23}$$

We insert into Eq. (23) the following complete sets of states:

$$\int d^3q\mid\mathbf{q}\rangle\langle\mathbf{q}\mid=1\ , \tag{24}$$

$$\sum_{m_n}\int d^3\kappa\mid\varphi^{[1/2]^{(-)}}_{\boldsymbol{\kappa},m_n}\rangle\langle\varphi^{[1/2]^{(-)}}_{\boldsymbol{\kappa},m_n}\mid=\begin{bmatrix}1&0\\0&1\end{bmatrix}\ , \tag{25}$$

and

$$\sum_{m_p}\chi^{[1/2]}_{m_p}\chi^{[1/2]^\dagger}_{m_p}=\begin{bmatrix}1&0\\0&1\end{bmatrix}\ . \tag{26}$$

Then, we get

$$\frac{1}{3}\sum_{\substack{m_6\\ m_n m_p}}\int d^3q\int d^3\kappa\langle\Psi^{[1]}_{m_6}\mid\varphi^{[1/2]^{(-)}}_{\boldsymbol{\kappa},m_n}\chi^{[1/2]}_{m_p}\mathbf{q}\rangle \times\langle\mathbf{q}\chi^{[1/2]}_{m_p}\varphi^{[1/2]^{(-)}}_{\boldsymbol{\kappa},m_n}\mid\Psi^{[1]}_{m_6}\rangle=1\ , \tag{27}$$

or, from Eq. (5),

$$\frac{1}{3}\sum_{\substack{m_6\\ m_n m_p}}\int d^3qd^3\kappa\mid A(\mathbf{q},\boldsymbol{\kappa};m_p,m_n,m_6)\mid^2=1\ . \tag{28}$$

Letting $m_p=m'_p$ and summing over m_p in Eq. (20) permits us to identify $V(\kappa,q)$ in Eq. (28). This identification leads to the sum rule of Eq. (22).

The power of the sum rule is that it serves as a constraint on the numerical calculations. The reader should note, however, that though the sum rule is exact within the framework of a three-body model, it must be used with care in interpreting experimental data since the three-body model does not allow for dissociation of the alpha particle. In the next section we see how it is used to assure the correctness of our results and to single out terms that contribute negligibly to $V(\kappa,q)$.

IV. NUMERICAL RESULTS

Five different models for the ground state of ^{6}Li will be considered in this series of papers. They are distinguished by the NN and αN interactions that underlie the three-body dynamics. The most elementary is the so-called simple model which was used in the first discussion of the alpha-deuteron structure of ^{6}Li from three-body models.[6] This model employs only an S-wave NN interaction and $P_{3/2}$ component of the αN interaction. The remaining four models are more sophisticated in that they include all the dominant components of the αN interaction at low energies, i.e., $S_{1/2}$, $P_{1/2}$, and $P_{3/2}$, and the NN interaction can have a tensor component. The four models are generated by two means: (1) The presence or absence of the tensor component in the NN interaction, and (2) whether the $S_{1/2}$ αN interaction is taken to be purely repulsive or to be an attractive interaction with the forbidden bound state removed.[5,7] These models are denoted as the repulsive- or attractive-projected, 0% or 4%, full models. The 0% and 4% denote the percentage of D state generated in the deuteron wave function by the tensor force. The parameters of the separable NN and αN interactions of these models can be found in Refs. 5 and 7, and their use in other applications in Refs. 1 and 8. Whatever model is used for the ground state of ^{6}Li, the corresponding αN parameters are used for the scattering state in the overlap. This assures full consistency of the calculations.

In order to make clear the numerical calculations presented in this section, it is necessary to examine $\mathcal{A}^{[\mathcal{L}]}_{M_\mathcal{L}}(K;\mathbf{q},\boldsymbol{\kappa})$ at the level where the spin part of the projections in Eqs. (14) and (16) have been carried out. $\mathcal{A}^{[\mathcal{L}]}_{M_\mathcal{L}}(K;\mathbf{q},\boldsymbol{\kappa})$ can be decomposed into three main parts according to the three terms of Eq. (17). We call these parts $X^{[\mathcal{L}]}$, $Y^{[\mathcal{L}]}$, and $Z^{[\mathcal{L}]}$, where $X^{[\mathcal{L}]}$ comes from the $G^{\ell'}(p_3)$ term, $Y^{[\mathcal{L}]}$ from the $F^{J'}_{\ell'(J\ell)}(p_1)$ term, and $Z^{[\mathcal{L}]}$ from the $F^{J'}_{\ell'(J\ell)}(p_2)$ term. Each has a plane-wave and scattered-wave contribution. Specifically,

$$X^{[\mathcal{L}]}_{M_{\mathcal{L}}}(K;\mathbf{q},\boldsymbol{\kappa})=4\pi\lambda_1 N\hat{1}\sum_{\substack{\ell,\ell'=0\\(\neq 1)}}^{2}\Bigg[\delta_{K1}\begin{Bmatrix}\mathcal{L}&\ell&\ell'\\1&1&1\end{Bmatrix}$$
$$\times\frac{g^1_\ell(|-\frac{1}{2}\boldsymbol{\kappa}-\frac{3}{5}\mathbf{q}|)G^{\ell'}(|\boldsymbol{\kappa}-\frac{4}{5}\mathbf{q}|)}{\bar{K}^2+\frac{5}{8}\kappa^2+\frac{3}{5}q^2}[Y^{[\ell]}(\widehat{-\tfrac{1}{2}\boldsymbol{\kappa}-\tfrac{3}{5}\mathbf{q}})\times Y^{[\ell']}(\widehat{\boldsymbol{\kappa}-\tfrac{4}{5}\mathbf{q}})]^{[\mathcal{L}]}_{M_{\mathcal{L}}}$$
$$+(-1)^{K+\mathcal{L}+1}\hat{1}^2\sum_U(-1)^U\hat{U}\sum_T(-1)^T\hat{T}\sum_{JL}(-1)^{J+L+1/2}\hat{J}^2$$
$$\times\begin{Bmatrix}\frac{1}{2}&\frac{1}{2}&U\\L&L&J\end{Bmatrix}\begin{Bmatrix}\frac{1}{2}&\frac{1}{2}&U\\K&1&\frac{1}{2}\end{Bmatrix}\begin{Bmatrix}T&\ell&\ell'\\1&1&1\end{Bmatrix}\begin{Bmatrix}K&1&\mathcal{L}\\T&U&1\end{Bmatrix}$$
$$\times\frac{2}{\pi}\frac{f_L^{J(-)^\dagger}(\kappa)}{h_L^J(\kappa)}\int d^2k_{23}\frac{h_L^J(k_{23})g^1_\ell(k_{12})G^{\ell'}(p_3)}{(k_{23}^2-\kappa^2-i\eta)(\bar{K}^2+\frac{5}{8}k_{23}^2+\frac{3}{5}q^2)}$$
$$\times[[Y^{[L]}(\hat{\mathbf{k}}_{23})\times Y^{[L]}(\hat{\boldsymbol{\kappa}})]^{[U]}$$
$$\times[Y^{[\ell]}(\hat{\mathbf{k}}_{12})\times Y^{[\ell']}(\hat{\mathbf{p}}_3)]^{[T]}]^{[\mathcal{L}]^\dagger}_{M_{\mathcal{L}}}\Bigg], \tag{29}$$

where under the integral $\mathbf{k}_{12}=\mathbf{k}_{23}-4\mathbf{q}/5$ and $\mathbf{p}_3=-\mathbf{k}_{23}/2-3\mathbf{q}/5$;

$$Y^{[\mathcal{L}]}_{M_{\mathcal{L}}}(K;\mathbf{q},\boldsymbol{\kappa})=\tfrac{5}{8}4\pi N\hat{1}\sum_{\substack{JJ'\\\ell\ell'}}\hat{J}\hat{J}'\frac{\Lambda^J_\ell h^J_\ell(\kappa)F^{J'}_{\ell'(J\ell)}(q)}{\bar{K}^2+\frac{5}{8}\kappa^2+\frac{3}{5}q^2}\begin{Bmatrix}\ell&\ell'&\mathcal{L}\\\frac{1}{2}&\frac{1}{2}&K\\J&J'&1\end{Bmatrix}[1+S^{JJ}_\ell(\kappa,q)][Y^{[\ell]}(\hat{\boldsymbol{\kappa}})\times Y^{[\ell']}(\hat{\mathbf{q}})]^{[\mathcal{L}]^\dagger}_{M_{\mathcal{L}}}, \tag{30}$$

where

$$S^{JJ}_\ell(\kappa,q)=(\bar{K}^2+\tfrac{5}{8}\kappa^2++\tfrac{3}{5}q^2)\frac{2}{\pi}\frac{f_\ell^{J(-)^\dagger}(\kappa)}{[h^J_\ell(\kappa)]^2}\int k_{23}^2dk_{23}\frac{[h^J_\ell(k_{23})]^2}{(k_{23}^2-\kappa^2-i\eta)(\bar{K}^2+\frac{5}{8}k_{23}^2+\frac{3}{5}q^2)}; \tag{31}$$

and

$$Z^{[\mathcal{L}]}_{M_{\mathcal{L}}}(K,\mathbf{q},\boldsymbol{\kappa})=\tfrac{5}{8}4\pi N\hat{1}(-1)^K\sum_{\substack{JJ'\\\ell\ell'}}\Bigg[(-1)^{\ell+1}\hat{J}\hat{J}'\begin{Bmatrix}\ell&\ell'&\mathcal{L}\\\frac{1}{2}&\frac{1}{2}&K\\J&J'&1\end{Bmatrix}\Lambda^J_\ell h^J_\ell(|-\tfrac{1}{5}\boldsymbol{\kappa}+\tfrac{24}{25}\mathbf{q}|)F^{J'}_{\ell'(J\ell)}(|-\boldsymbol{\kappa}-\tfrac{1}{5}\mathbf{q}|)$$
$$\times[Y^{[\ell]}(\widehat{-\tfrac{1}{5}\boldsymbol{\kappa}+\tfrac{24}{25}\mathbf{q}})\times Y^{[\ell']}(\widehat{-\boldsymbol{\kappa}-\tfrac{1}{5}\mathbf{q}})]^{[\mathcal{L}]^\dagger}_{M_{\mathcal{L}}}$$
$$+(-1)^{\mathcal{L}}\sum_U(-1)^U\hat{U}\sum_S\hat{S}^2\sum_T\hat{T}\sum_{\mathscr{J}L}(-1)^{\mathscr{J}+L+3/2}\hat{\mathscr{J}}^2$$
$$\times\begin{Bmatrix}\frac{1}{2}&\frac{1}{2}&U\\L&L&\mathscr{J}\end{Bmatrix}\begin{Bmatrix}\frac{1}{2}&\frac{1}{2}&U\\K&S&\frac{1}{2}\end{Bmatrix}\begin{Bmatrix}K&1&\mathcal{L}\\T&U&S\end{Bmatrix}$$
$$\times(-1)^\ell\hat{J}\hat{J}'\begin{Bmatrix}\ell&\frac{1}{2}&J\\\ell'&\frac{1}{2}&J'\\T&S&1\end{Bmatrix}\frac{2}{\pi}\frac{f_L^{\mathscr{J}(-)^\dagger}(\kappa)}{h_L^{\mathscr{J}}(\kappa)}\Lambda^J_\ell$$
$$\times\int d^3k_{23}\frac{h_L^{\mathscr{J}}(k_{23})h^J_\ell(k_{31})F^{J'}_{\ell'(J\ell)}(p_2)}{(k_{23}^2-\kappa^2-i\eta)(\bar{K}^2+\frac{5}{8}k_{23}^2+\frac{3}{5}q^2)}$$
$$\times[[Y^{[L]}(\hat{\mathbf{k}}_{23})\times Y^{[L]}(\hat{\boldsymbol{\kappa}})]^{[U]}$$
$$\times[Y^{[\ell}(\hat{\mathbf{k}}_{31})\times Y^{[\ell']}(\hat{\mathbf{p}}_2)]^{[T]}]^{[\mathcal{L}]^\dagger}_{M_{\mathcal{L}}}\Bigg], \tag{32}$$

where under the integral $\mathbf{k}_{31}=-\mathbf{k}_{23}/5+24\mathbf{q}/25$ and $\mathbf{p}_2=-\mathbf{k}_{23}-\mathbf{q}/5$. The two quantum numbers upon which $\mathcal{A}$ and thus X, Y, and Z, depend, namely K and $\mathcal{L}$, represent the total spin angular momentum of the neutron and proton in the final state and the total orbital angular momentum in the final state generated by the motion of the proton relative to the nα c.m. and the relative motion of the neutron and alpha particle, respectively. Since the overlap of the final state is with the ^{6}Li ground state (1^+), K and $\mathcal{L}$ must couple to unity.

Now, from Eqs. (29)–(32) it is even more apparent than before that the calculation of $V(\kappa,q)$ is very tedious. The formulas involve many $6J$ and $9J$ coefficients, complex arithmetic, and complicated spherical harmonic couplings. Thus, the sum rule of Eq. (22) is the key to assuring correct results. In order to ascertain the dominant contributions to $V(\kappa,q)$, the sum rule is applied in stages.

It is tempting to hope that only the $\mathcal{L}=0$ contribution to $V(\kappa,q)$ will be significant, especially since it reduces the complexity of the coupling in Eq. (21). Thus, we start by including only the $\mathcal{L}=0$ partial wave.[9] When only the plane-wave contribution to $\mathcal{A}^{[0]}$ is considered, the sum rule yields 0.898 for the full (4%) repulsive model. This seems like a promising result. However, when both the plane-wave and scattered-wave pieces are included, i.e., using the complete $\mathcal{A}^{[0]}$, we get a significantly lower sum-rule value: 0.629. This is clear evidence that part of the scattering contribution is missing; apparently, contributions from the $\mathcal{L}\neq 0$ amplitudes make up for the destructive interference that occurs between the plane-wave and scattered wave contributions when $\mathcal{L}=0$.

The essential role of the $\mathcal{L}\neq 0$ partial waves, in general, is especially striking if only the Y part of $\mathcal{A}^{[\mathcal{L}]}$ is considered. The contribution to the sum rule for this case comes from

$$\tfrac{1}{3}\sum_{\substack{K\\ \mathcal{L}}}\hat{K}^2\hat{\mathcal{L}}\frac{1}{4\pi}\int d\Omega_q\int d\Omega_\kappa[\bar{Y}^{[\mathcal{L}]}(K;\mathbf{q},\boldsymbol{\kappa})\times Y^{[\mathcal{L}]}(K;\mathbf{q},\boldsymbol{\kappa})]^{[0]}$$

$$=\frac{1}{4\pi}\sum_{\substack{JJ'\\ \ell\ell'}}\left[\frac{5}{8}\frac{4\pi}{\bar{K}^2+\frac{5}{8}\kappa^2+\frac{3}{5}q^2}\right]^2[\Lambda^J_\ell h^J_\ell(\kappa)F^{J'}_{\ell'(J\ell)}(q)]^2[1+S^{JJ}_\ell(\kappa,q)+\bar{S}^{JJ}_\ell(\kappa,q)+|S^{JJ}_\ell(\kappa,q)|^2]\ . \quad (33)$$

For the sum rule to be satisfied, i.e., produce the same value as the plane-wave result, the scattering terms must cancel after integration over κ and q. That they do cancel can be seen from the arguments given in the Appendix. If the sum over $\mathcal{L}$ does not cover its full range of values, then uncanceled cross terms appear on the right-hand side of Eq. (33), e.g.,

$$F^{J'}_{\ell'(J\ell)}(q)F^{\bar{J}'}_{\ell'(\bar{J}\ell)}(q)S^{JJ}_\ell(\kappa,q)\bar{S}^{\bar{J}\bar{J}}_\ell(\kappa,q)\ ,$$

TABLE I. Plane-wave component contributions (≥1% total) to sum rule according to partial wave. (cr) means cross term, i.e., the (2,31) term with the (1,23) term. Full (4%) repulsive model. Contributions in percent.

Component	$\mathcal{L}=0$	$\mathcal{L}=1$	$\mathcal{L}=2$	Total
$G^0\times G^0$	45.10		3.49	48.59
$G^0\times F^{1/2}_{0[(1/2)0]}$	−21.71			−21.71
$G^0\times F^{3/2}_{1[(1/2)1]}$	5.19		0.48	5.67
$G^0\times F^{1/2}_{1[(3/2)1]}$	9.01		0.80	9.81
$G^0\times F^{3/2}_{1[(3/2)1]}$	16.18		−1.17	15.01
$F^{1/2}_{0[(1/2)0]}\times F^{1/2}_{0[(1/2)0]}$	3.08			3.08
$F^{3/2}_{1[(1/2)1]}\times F^{3/2}_{1[(1/2)1]}$	0.44	0.90	0.14	1.48
$F^{1/2}_{1[(3/2)1]}\times F^{1/2}_{1[(3/2)1]}$	1.71	3.39	0.53	5.63
$F^{3/2}_{1[(3/2)1]}\times F^{3/2}_{1[(3/2)1]}$	5.41	8.11	1.08	14.60
$F^{1/2}_{0[(1/2)0]}\times F^{1/2}_{0[(1/2)0]}$ (cr)	2.87			2.87
$F^{3/2}_{1[(3/2)1]}\times F^{3/2}_{1[(3/2)1]}$ (cr)	3.49	5.38	0.69	9.56
$F^{1/2}_{0[(1/2)0]}\times F^{3/2}_{1[(3/2)1]}$	0.37			0.37
$F^{1/2}_{1[(3/2)1]}\times F^{3/2}_{1[(1/2)1]}$	2.91	0.44	0.90	4.25
	74.05	18.22	6.94	99.21
All other terms	17.77	−13.62	−3.44	0.71
	91.82	4.60	3.50	99.92

TABLE II. Plane-wave component contributions ($\geq 1\%$ total) to sum rule according to partial wave. (cr) means cross term, i.e., the (2,31) term with the (1,23) term. Full (4%) attractive-projected model. Contributions in percent.

Component	$\mathcal{L}=0$	$\mathcal{L}=1$	$\mathcal{L}=2$	Total
$G^0\times G^0$	42.00		3.10	45.10
$G^0\times F^{1/2}_{0[(1/2)0]}$	−22.78			−22.78
$G^0\times F^{3/2}_{1[(1/2)1]}$	4.88		0.41	5.29
$G^0\times F^{1/2}_{1[(3/2)1]}$	8.33		0.66	8.99
$G^0\times F^{3/2}_{1[(3/2)1]}$	16.10		−1.00	15.10
$F^{1/2}_{0[(1/2)0]}\times F^{1/2}_{0[(1/2)0]}$	5.07			5.07
$F^{3/2}_{1[(1/2)1]}\times F^{3/2}_{1[(1/2)1]}$	0.42	0.87	0.13	1.42
$F^{1/2}_{1[(3/2)1]}\times F^{1/2}_{1[(3/2)1]}$	1.60	3.23	0.50	5.33
$F^{3/2}_{1[(3/2)1]}\times F^{3/2}_{1[(3/2)1]}$	5.85	8.78	1.17	15.80
$F^{1/2}_{0[(1/2)0]}\times F^{1/2}_{0[(1/2)0]}$ (cr)	3.65			3.65
$F^{3/2}_{1[(3/2)1]}\times F^{3/2}_{1[(3/2)1]}$ (cr)	3.75	5.90	0.74	10.39
$F^{1/2}_{0[(1/2)0]}\times F^{3/2}_{1[(3/2)1]}$	1.10			1.10
$F^{1/2}_{1[(3/2)1]}\times F^{3/2}_{1[(1/2)1]}$	2.74	0.38	0.82	3.94
	72.71	19.16	6.53	98.40
All other terms	18.59	−14.15	−2.99	1.45
	91.30	5.01	3.54	99.85

etc. Such terms can lead to contributions that destroy the sum rule. Moreover, it is clear that when the scattering contributions are present $\mathcal{L}$ may have to range over all its values for saturation of the sum rule. With this in mind, let us systematically look at the sum rule beginning with the pure plane-wave contributions.

The plane-wave results for the full (4%) repulsive- and attractive-projected models are given in Tables I and II, respectively.[10] The wave-function-component contributions that are explicitly singled out agree *in total* with the component contributions to the wave function normalization given in the Parke-Lehman paper of Ref. 1. This is as it must be. Small differences that occur are numerical in origin due to the fact that here the calculation is done from the plane-wave contribution to the $^6\mathrm{Li}\rightarrow \mathrm{p}+(\mathrm{n}\alpha)$ overlap amplitude. As a consequence, the coordinates are not the optimal set used for the normalization calculation in Ref. 1, but the set appropriate for the $\mathrm{p}+(\mathrm{n}\alpha)$ configuration. Thus, angle dependencies that were removed by a change of variables in the normalization calculation remain in the plane-wave sum-rule calculation. This makes the numerical integration more sensitive to the integration mesh. Nevertheless, the calculations for the component totals are accurate to better than $\pm 0.07\%$ on the average.

TABLE III. ^{6}Li L-S orbital probabilities in percent.

Model	$^3S_1$ ($\mathcal{L}=0$)	$^3P_1+{}^1P_1$ ($\mathcal{L}=1$)	$^3D_1$ ($\mathcal{L}=2$)	Total
		Full (4%) repulsive		
Ref. 8	91.78	4.51	3.71	100.00
This work	91.82	4.60	3.50	99.92
		Full (4%) attractive-projected		
Ref. 8	91.47	5.13	3.40	100.00
This work	91.30	5.01	3.54	99.85

What should be noted from Tables I and II, besides the fact that the sum rule is satisfied, is the partial-wave decompositon in $\mathcal{L}$. It is striking that the terms in the normalization calculation of Ref. 1 that are considered to be small end up that way through the $\mathcal{L}=0$ contribution being canceled by the $\mathcal{L}=1$ and 2 contributions (see "all other terms" in Tables I and II). Furthermore, the $\mathcal{L}$ decomposition with only plane waves corresponds to the L-S coupling projection of the ground-state wave function where the $^3P_1$ and $^1P_1$ contributions are summed. We see (Table III), upon comparison with the L-S coupling results obtained directly from the wave function,[8] that the $\mathcal{L}$-partial-wave sums are accurate to better than $\pm 0.15\%$ on the average.

Now that it is clear that the full plane-wave amplitude satisfies the sum rule and that more than the $\mathcal{L}=0$ partial wave is required to saturate the sum rule when the $\mathrm{n}\alpha$ rescattering is present; we now look at adding the rescattering contributions systematically. To see what is involved, we list in Table IV the allowed values for the quantum numbers in the sums for $X^{[\mathcal{L}]}$, $Y^{[\mathcal{L}]}$, and $Z^{[\mathcal{L}]}$. There are many terms, some of which involve complicated spherical harmonic couplings. The approach is to add to the plane-wave amplitudes those $\mathcal{L}=1$ and 2 rescattering contributions that are significant, working with the largest wave-function components first and from the simplest to the more complicated couplings, until the sum rule is approximately saturated. The complications arise in the X and Z terms themselves, and through the X-Y, X-Z, etc. cross terms, because the Y term alone is quite elegant in its form [see Eq. (33)].

The rationale as to the terms retained in the calculation of $V(\kappa,q)$ can be outlined as follows: Though all

TABLE IV. Allowed quantum numbers in the sums that determine the overlap amplitude ($\mathcal{L} > 0$).

	$X^{[\mathcal{L}]}$										$Y^{[\mathcal{L}]}$										$Z^{[\mathcal{L}]}$									
$\mathcal{L}=1$ plane wave																														
ℓ						2								1										1						
ℓ'						2								1										1						
$\mathcal{L}=2$ plane wave																														
ℓ					0	2	2						0	1	1								0	1	1					
ℓ'					2	0	2						2	1	3								2	1	3					
$\mathcal{L}=1$ scattered wave																														
U		1	1	1	0	0	1	1	1								1	1	1	0	0	1	1	1						
T		0	2	2	1	1	0	1	2								0	2	0	1	1	1	2	2						
L		1	1	1	0	1	1	1	1								1	1	1	0	1	1	1	1						
ℓ		0	0	2	2	2	2	2	2					1			0	0	1	1	1	1	1	1						
ℓ'		0	2	0	2	2	2	2	2					1			0	2	1	1	1	1	1	3						
$\mathcal{L}=2$ scattered wave																														
U	0	0	1	0	0	1	0	0	1	1	1					0	0	1	0	0	1	1	0	0	1					
T	2	2	2	2	2	2	2	2	1	2	3					2	2	2	2	2	1	2	2	2	2					
L	0	1	1	0	1	1	0	1	1	1	1					0	1	1	0	1	1	1	0	1	1					
ℓ	0	0	0	2	2	2	2	2	2	2	2	0	1	1		0	0	0	1	1	1	1	1	1	1					
ℓ'	2	2	2	0	0	0	2	2	2	2	2	2	1	3		2	2	2	1	1	1	1	3	3	3					

contributions from the Y term are retained, it is noted that the $\mathcal{L}=2$ partial-wave contribution is very small. For example, in the region of the $P_{3/2}$ α-n resonance, i.e., $E_\kappa = 0.7$ MeV and $q = 0.4$ fm^{-1}, the contribution to $V(\kappa,q)$ from Y alone equals 19.54 fm^6, of which only 0.10 fm^6 comes from $\mathcal{L} \equiv 2$. Moreover, a calculation of all the $U=0$ pieces of the $\mathcal{L}=2$ contribution (see Table IV) indicated that their total is insignificant compared to the $\mathcal{L}=0$ total. On the basis of these results and the fact that the L-S coupling D-state component ($\mathcal{L}=2$) in the ground-state wave function has probability less than 4%, it was decided to omit the $\mathcal{L}=2$ contributions, except the Y term, and add all the nonnegligible $\mathcal{L}=1$ pieces. The reader should keep in mind that a few percent missing from the sum-rule integral means only a fraction of a percent error in the value of $V(\kappa,q)$, at a given κ and q, in general.

Consider $V(\kappa,q)$ in the vicinity of its maximum value, i.e., $E_\kappa = 0.7$ MeV and $q = 0.4$ fm^{-1}. We see from Table V that the $\mathcal{L}=0$ contribution is 100.42 fm^6. The nonnegligible $\mathcal{L}=1$ terms add another 38.4 fm^6 (see Table VI). Two observations are in order with regard to the $\mathcal{L}=1$ contributions. No significant contributions arise from the G^2 spectator function in X and most of the terms that contain the g_2^1 form factor from the tensor part of the NN interaction are negligible. A detailed account of these considerations can be found in Ref. 4.

How does the sum rule turn out with neglect of the indicated terms? As can be see in Table VII, the answer is quite well. Only about 5% is missing from the sum-rule value *and* the plane-wave-only result compared with the value when the scattered wave is included turn out to be equal. Thus, the calculation is essentially complete, while being consistent. Furthermore, the level of sensitivity to the integration meshes in the sum-rule calculation can be seen from Table VII. The numbers in

TABLE V. $\mathcal{L}=0$ contribution to $V(\kappa,q)$ at $E_\kappa = 0.7$ MeV and $q = 0.4$ fm^{-1} [full (4%) repulsive model].

Term	$V(\kappa,q)$ (fm^6)
$X \times X$	22.16
$Y \times Y$	13.11
$Z \times Z$	4.23
$X \times Y$	29.12
$X \times Z$	16.96
$Y \times Z$	14.84
Total	100.42

TABLE VI. $\mathcal{L}=0$ and non-negligible $\mathcal{L}=1$ contributions to $V(\kappa,q)$ at $E_\kappa = 0.7$ MeV and $q = 0.4$ fm^{-1} [full (4%) repulsive model].

Term	$V(\kappa,q)$ (fm^6)
$\mathcal{L}=0$ (all terms)	100.4
$X^{[1]}(g_0^1 G^0) \times X^{[1]}(g_0^1 G^0)$	5.6
$X^{[1]}(g_0^1 G^0) \times X^{[1]}(g_2^1 G^0)$	0.0
$X^{[1]}(g_0^1 G^0) \times Y^{[1]}$	11.1
$X^{[1]}(g_2^1 G^0) \times Y^{[1]}$	0.1
$X^{[1]}(g_0^1 G^0) \times Z^{[1]}$	5.7
$Y^{[1]} \times Y^{[1]}$	6.4
$Y^{[1]} \times Z^{[1]}$	7.0
$Z^{[1]} \times Z^{[1]}$	2.4
$Y^{[2]} \times Y^{[2]}$	0.1
Total	138.8

TABLE VII. Sum rule results [full (4%) repulsive model].

Case		Sum rule value
	Plane-wave only	
$\mathcal{L}=0$	(16–6/563)	0.898
	(16–10/563)	0.913
	(24–10/563)	0.915
$\mathcal{L}=0,1$	(16–6/563)	0.943
	(24–10/563)	0.959
	(16–6/620)	0.946
$\mathcal{L}=0,1,2$	(Y only)	0.128
	Scattered-wave included	
$\mathcal{L}=0,1$	(16–6/563)	0.946
	(24–10/563)	0.959
$\mathcal{L}=0,1,2$	(Y only)	0.125

parentheses give, in order, the number of points in all infinite integrations except that over κ (or $E_\kappa=5\kappa^2/8M$), the number of points in the angular integrations, and the number of points in the κ integration. They are performed with Gegenbauer, Gaussian, and variable-interval trapezoidal quadrature, respectively.

Finally, with the validity of our calculation of $V(\kappa,q)$ established, we give in Figs. 2 and 3 plots of $V(\kappa,q)$ for two of the models under consideration: full (4%) repulsive $S_{1/2}$ and full (4%) attractive-projected $S_{1/2}$ models, respectively.

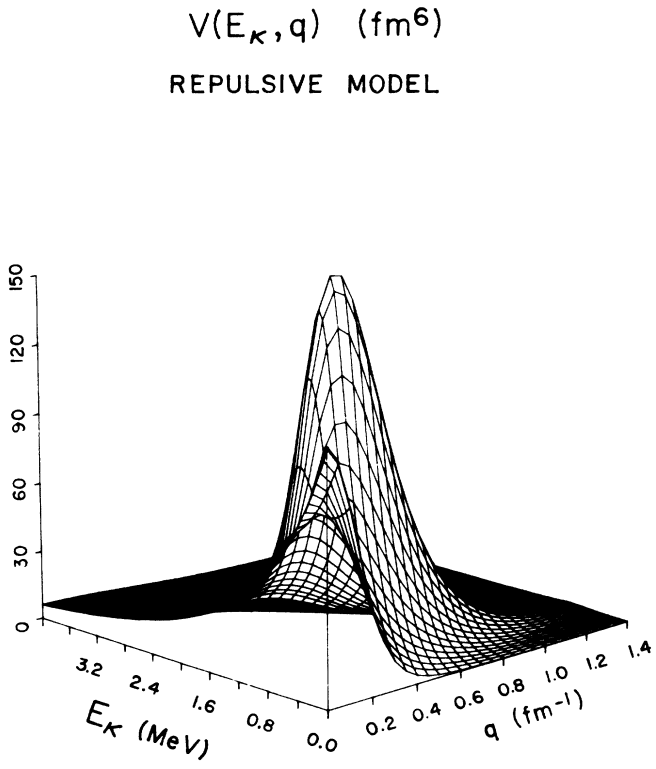

FIG. 2. ^{6}Li$\rightarrow$p + (nα) joint momentum distribution. Full (4%) repulsive $S_{1/2}$ model.

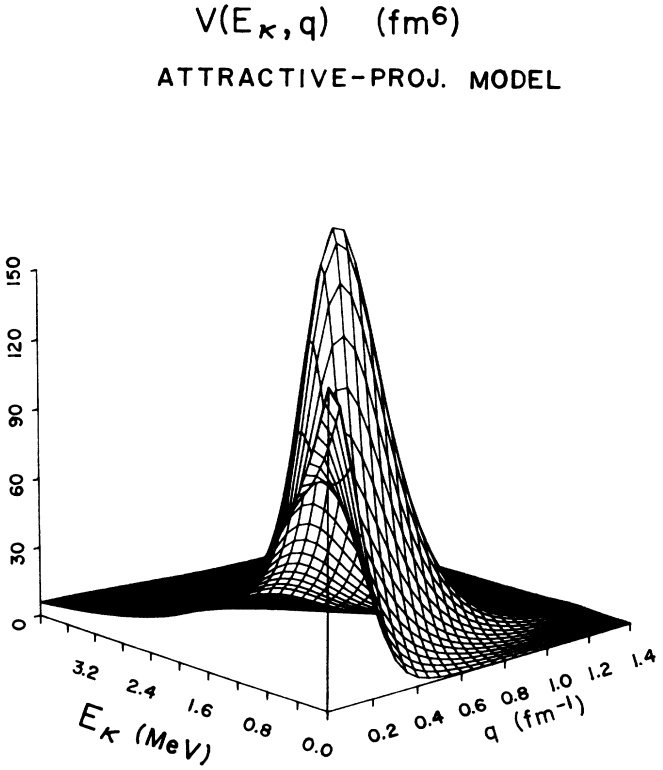

FIG. 3. ^{6}Li$\rightarrow$p + (nα) joint momentum distribution. Full (4%) attractive-projected $S_{1/2}$ model.

V. DISCUSSION

The physics contained in the three-body model of the ^{6}Li$\rightarrow$p + (nα) vertex is embedded in the joint momentum distribution $V(\kappa,q)$. As mentioned above, $V(\kappa,q)$ gives the probability of finding within ^{6}Li a proton moving with momentum of magnitude q relative to the c.m. of an interacting nα pair that has relative momentum of magnitude κ per unit momentum volume per unit momentum cubed. $V(\kappa,q)$ is the central object in the interpretation of data from coincidence reactions like ^{6}Li(p,2p)nα or ^{6}Li(e,e'p)nα. Therefore, our aim is to understand its content, based on three-body dynamics, as completely as possible.

From the results displayed in Figs. 2 and 3, it is immediately apparent that $V(\kappa,q)$, plotted as $V(E_\kappa,q)$, where $E_\kappa=5\kappa^2/8M$ is the relative energy of the nα pair, has interesting structure. Two aspects of $V(E_\kappa,q)$ are most notable: (1) the prominent peak at $E_\kappa\sim0.7$–0.8 MeV and $q\sim0.35$ fm^{-1}, and (2) the nonzero value at $q=0$ as a function of E_κ. The large maximum of $V(E_\kappa,q)$ occurs due to the strong rescattering of the nα pair in the resonant $P_{3/2}$ partial wave. This resonant contribution is superimposed on the "background" from rescattering in the $S_{1/2}$ and $P_{1/2}$ partial waves. The excitation energy of this resonant-rescattering peak in $V(E_\kappa,q)$ is essentially the energy at which the $P_{3/2}$ resonance occurs in free nα scattering. The location of the peak with respect to the value of q is controlled by the dynamics of the three-body model of the ^{6}Li ground

state; that is, by all the underlying two-body interactions. Starting from the resonant peak and approaching the origin, $V(E_\kappa,q)$ goes through a saddle point and a secondary maximum is reached at $E_\kappa=0$ and $q=0$. For $q=0$, but $E_\kappa\neq 0$, we find $V(E_\kappa,q)\neq 0$. The fact that $V(E_\kappa,q)$ is not zero in this latter region is due to the nα rescattering in the final state in a relative S wave, coming both from the plane- and rescattered-wave pieces, that has a nonzero overlap with components of the same angular momentum in the ^{6}Li ground-state wave function. These components are generated by the three-body dynamics from the given NN and Nα interactions. Let us look at this point in more detail.

In Fig. 4 we give $V(\kappa,q)$ for fixed κ, $E_\kappa=0.7$ MeV, as a function of q. When the nα scattering in the final state is removed, we see that the prominent resonant peak disappears and the value of $V(\kappa,q)$ rises at the origin. The plane-wave version of $V(\kappa,q)$ continually decreases from a maximum at $q=0$. Addition of the nα-scattering contributions to the plane-wave term leads to the prominent $P_{3/2}$ resonance and reduction of the value of $V(\kappa,q)$ at $q=0$. The $S_{1/2}$ rescattering term interferes *destructively* with the $S_{1/2}$ partial-wave piece of the plane-wave term. This is the case because the P-wave contributions, whether they come from the plane-wave or rescattered-wave terms, are identically zero at $q=0$.[11] Therefore, removal of only the $S_{1/2}$ component of the nα scattering will lead to a value of $V(\kappa,q)$ at $q=0$ equal to the plane-wave result. Clearly, the $S_{1/2}$ nα interaction plays a major role in the physics of the final state.

How does it come about that final-state nα S-wave components have a nonzero overlap with the three-body ^{6}Li ground-state wave function? First, we observe that

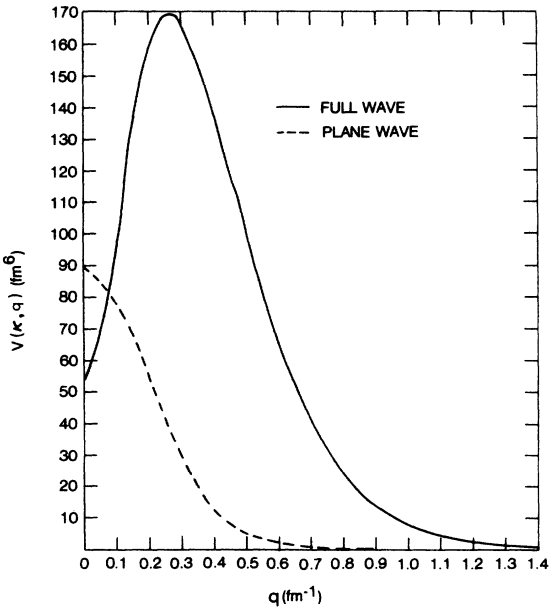

FIG. 4. ^{6}Li→p + (nα) joint momentum distribution at $E_\kappa=0.7$ MeV. Full (4%) repulsive $S_{1/2}$ model.

due to the unit total angular momentum and positive parity of the ^{6}Li ground state, the only nα S-wave components that can possibly overlap with the ground state have the proton moving relative to the nα c.m. with either S-wave or D-wave angular momentum. At $q=0$, the D wave yields zero contribution to $V(\kappa,q)$. Thus, there must be compatible components in the ^{6}Li ground-state wave function that can overlap with an $S_{1/2}$ nα pair with an S-wave proton moving relative to the nα c.m. If we were to construct a pure p-shell model of the ^{6}Li ground state with an inert alpha-particle core, there would be no overlap, i.e., $V(\kappa,q)\equiv 0$. On the other hand, as can be seen from Eq. (17), the three-body model has three types of nonorthogonal components in its wave function: (1) α-(np), (2) p-(nα), and (3) n-(pα). So, even if the $S_{1/2}$ nα interaction (also used for pα) is removed from the dynamics of the ground state, there will be a nonzero overlap at $q=0$ with the $S_{1/2}$ nα component of the final state whether the final state includes the scattered wave or not. This occurs because of components (1) and (3) in the ground-state wave function [component (3) because its permutation of particles is different from (2)]. For example, when the alpha-particle moves with S-wave angular momentum relative to the c.m. of an S-wave np pair, such a configuration contains a projection corresponding to an S-wave proton moving relative to the c.m. of an S-wave nα pair. Nevertheless, as one might expect, dropping the $S_{1/2}$ component of the nα interaction in the dynamics of the ground state significantly alters the results (this will be shown in the planned second paper of this series).

To more fully illustrate the role of the $S_{1/2}$ nα interaction in the final state, we introduce the proton momentum distribution in ^{6}Li:

$$\rho(q)=\int_{E_{\kappa_{\min}}}^{E_{\kappa_{\max}}}\mu_{n\alpha}\kappa V(\kappa,q)dE_\kappa\ , \tag{34}$$

where $\mu_{n\alpha}=4M/5$. [Note that the integrand is the ^{6}Li→p + (nα) spectral function as defined directly following Eq. (21).] $\rho(q)$ is given in Fig. 5 for $E_{\kappa_{\min}}=0$ and $E_{\kappa_{\max}}=2.5$ MeV for the full (4%) repulsive $S_{1/2}$ model. This range of E_κ encompasses the peak due to the $P_{3/2}$ nα resonance. Beginning with the plane-wave calculation, we note that it has a maximum at $q=0$ and falls steadily with increasing q. That is what was observed in Fig. 4 at a fixed E_κ. When only the $S_{1/2}$ partial wave of the rescattering contribution is added, destructive interference occurs such that $\rho(q)$ is lowered in value, but it retains the same general shape. The $S_{1/2}$ scattered-wave contribution interferes destructively with the $S_{1/2}$ plane-wave contribution. If the plane-wave amplitude is removed, the $S_{1/2}$ scattered-wave amplitude alone leads to a small $\rho(q)$. The combined result is almost like the difference of the plane-wave $\rho(q)$ and the $S_{1/2}$ scattered-wave $\rho(q)$. Of course, it is more complicated than a simple difference since the plane-wave amplitude is real and the $S_{1/2}$ scattered-wave amplitude is complex. Finally, when the $P_{1/2}$ and $P_{3/2}$ scattered-wave contributions are added, $\rho(q)$ has a minimum at $q=0$ since partial waves of nonzero angular momentum contribute nothing at

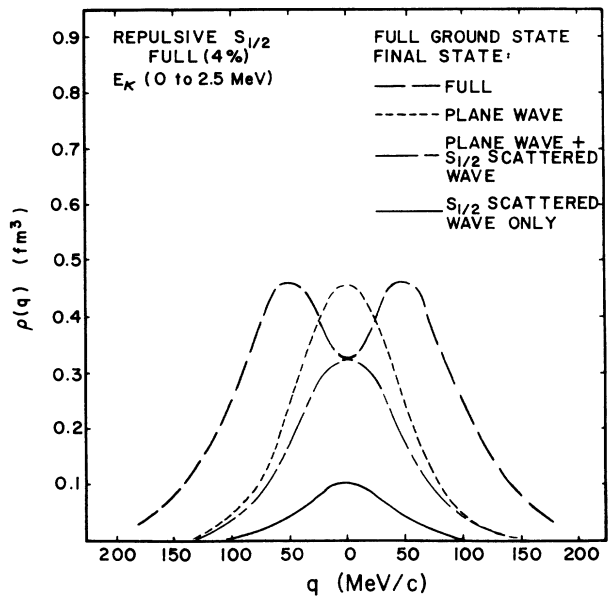

FIG. 5. ^{6}Li→p + (nα) proton momentum distribution for $0 \leq E_\kappa \leq 2.5$ MeV. Full (4%) repulsive $S_{1/2}$ model.

$q=0$ and add to $\rho(q)$ for $q \neq 0$.

The three-body approach to the ^{6}Li→p + (nα) vertex has led us to a deeper understanding of the underlying physics. Some aspects of this physics were already understood with the alpha-deuteron cluster approach of Saito, Hiura, and Tanaka, where they allowed for the unbound ^{5}He in the final state.[12] Based on the limited variational approach to the three-body model of ^{6}Li then available,[13] Saito *et al.* were under the mistaken impression that the three-body model of ^{6}Li was inadequate as far as its content of components that have nonzero overlap with an $S_{1/2}$ nα pair, while the proton *has* S-wave relative motion with respect to the nα c.m. The present work shows that the three-body model derived by exact (numerical) solution of Schrödinger's equation with $^3S_1$-$^3D_1$ NN and $S_{1/2}$, $P_{1/2}$, and $P_{3/2}$ Nα interactions as input leads to a comprehensive description of the ^{6}Li→p + (nα) vertex. In the next two papers in this series, these results will be confronted with available experimental data for the ^{6}Li(p,2p)nα and ^{6}Li(e,e'p)nα reactions to test the viability of the model. The success of such comparisons is important since no adjustable parameters are involved. As mentioned above, the model already is known to describe well ^{6}Li static properties[1,8] and especially the ^{6}Li→α + d momentum distribution.[1] The correct description of the ^{6}Li→α + d vertex in the three-body model has its origin in the dynamics of the underlying $S_{1/2}$ nα interaction, that partial wave of the nα interaction that makes manifest the Pauli exclusion between the n and α. In the α-d cluster model of Saito *et al.*, the 2*s* character of the effective α-d wave function is built into the wave function to satisfy the Pauli principle. In contrast, the three-body approach is fixed once the underlying two-body interactions are specified, and the 2*s* character of the effective α-d wave function in ^{6}Li is a prediction. Moreover, it is apparent that once the ^{6}Li ground-state wave function has components that have a nonzero overlap with a proton moving in an S-wave relative motion, the proton momentum distribution will be nonzero at $q=0$ even if all particles are noninteracting in the final state. When the nα pair in the final state interact in the dominant $S_{1/2}$, $P_{1/2}$, and $P_{3/2}$ partial waves, the proton momentum distribution changes shape from the plane-wave result, which has a maximum at $q=0$, to a shape where $q=0$ is a relative (nonzero) minimum and the maximum occurs at $q \sim 50$ MeV/*c*. The S-wave components in the ground state of ^{6}Li "fill" the minimum in the proton momentum distribution compared to a *p*-shell shell model of ^{6}Li *and* the $S_{1/2}$ nα interaction in the final state controls the shape to have a relative minimum at $q=0$, rather than a maximum, as it would have if the nα system did not interact or interacted only in P waves.

VI. SUMMARY AND CONCLUSION

In the first of this planned series of three papers on a three-body description of the ^{6}Li→p + (nα) vertex, we developed the underlying formalism. The key physical quantity is the ^{6}Li→p + (nα) joint momentum distribution which gives the probability of finding a proton with momentum q relative to the c.m. of an nα pair that possess relative momentum κ per momentum space volume per unit momentum cubed. We showed that the joint momentum distribution satisfies a sum rule, consistent with its probability interpretation, that follows from the normalization of the ^{6}Li wave function and the completeness of the p + (nα) states. The sum rule was used to assure the correctness of the calculation of the joint momentum distribution and to eliminate terms that contribute insignificantly. In assessing the physics of the joint momentum distribution, we were led to define the valence-proton momentum distribution in ^{6}Li. From numerical calculations of these two distributions with specific three-body models, we find that the three-body approach leads to a deeper understanding of the underlying physics. For example, the three-body model of ^{6}Li generates pure S-wave components in the ^{6}Li ground-state wave function. As a consequence, a state with a proton moving in an S-wave relative to the nα c.m., while the nα pair has S-wave relative motion, has nonzero overlap with the ^{6}Li ground state of three-body models. This is in contrast to a *p*-shell shell model of ^{6}Li with an inert alpha-particle core. The three-body model leads to the joint momentum distribution being nonzero at $q=0$ for any nα excitation energy. Thus, the proton momentum distribution has a nonzero value at $q=0$: A maximum at $q=0$ if the final-state p-(nα) system is totally noninteracting or a relative minimum at $q=0$ when the nα interactions are present. The relative minimum is due to destructive interference between the plane-wave and scattered-wave terms of the nα wave function.

The work of the authors was supported in part by the U.S. Department of Energy under Grant No. DE-FG05-86-ER40270.

APPENDIX

The purpose of this Appendix is to demonstrate the completeness of the αn-scattering-state wave functions as given by Eq. (9). First, we observe that

$$\delta^3(\mathbf{k}-\boldsymbol{\kappa})=\frac{\delta(k-\kappa)}{k^2}\sum_{\ell m} Y_m^{[\ell]}(\hat{\mathbf{k}})Y_m^{[\ell]\dagger}(\hat{\boldsymbol{\kappa}}) \tag{A1}$$

and

$$\sum_{m_n}\chi_{m_n}^{[1/2]}\chi_{m_n}^{[1/2]\dagger}=\begin{bmatrix}1&0\\0&1\end{bmatrix}\equiv I\ , \tag{A2}$$

so that by recoupling

$$\delta^3(\mathbf{k}-\boldsymbol{\kappa})I=\frac{\delta(k-\kappa)}{k^2}\times\sum_{J\ell}(-1)^{2J}\hat{J}[\mathcal{Y}_\ell^{[J]}{}_{1/2}(\hat{\mathbf{k}})\times\tilde{\mathcal{Y}}_\ell^{[J]}{}_{1/2}(\hat{\boldsymbol{\kappa}})]^{[0]}\ . \tag{A3}$$

Then, Eq. (A3) can be used to rewrite Eq. (9) as

$$\varphi_{\kappa,m_n}^{[1/2]^{(-)}}(\mathbf{k})=\sum_{J\ell}(-1)^{2J}\hat{J}\Delta_\ell^{(-)}(k,\kappa)[\mathcal{Y}_\ell^{[J]}{}_{1/2}(\hat{\mathbf{k}})\times\tilde{\mathcal{Y}}_\ell^{[J]}{}_{1/2}(\hat{\boldsymbol{\kappa}})]^{[0]}\chi_{m_n}^{[1/2]}\ , \tag{A4}$$

where

$$\Delta_\ell^{J(-)}(k,\kappa)=\frac{\delta(k-\kappa)}{k^2}+\frac{1}{2\pi^2}\frac{4\pi}{k^2-\kappa^2+i\eta}\frac{h_\ell^J(k)}{h_\ell^J(\kappa)}f_\ell^{J(-)}(\kappa)\ , \tag{A5}$$

and $f_\ell^{J(-)}(\kappa)$ is nonzero only for the $S_{1/2}$, $P_{1/2}$, and $P_{3/2}$ partial waves. Therefore, after further recoupling, the completeness integral can be written as

$$\sum_{m_n}\int d^3\kappa\,\varphi_{\kappa,m_n}^{[1/2]^{(-)}}(\mathbf{k})\varphi_{\kappa,m_n}^{[1/2]^{(-)\dagger}}(\mathbf{k}')=\sum_{J\ell}\left[\int_0^\infty\kappa^2 d\kappa[\Delta_\ell^{J(-)}(k,\kappa)\Delta_\ell^{J(-)*}(k',\kappa)]\right][(-1)^{2J}\hat{J}[\mathcal{Y}_\ell^{[J]}{}_{1/2}(\hat{\mathbf{k}})\times\tilde{\mathcal{Y}}_\ell^{[J]}{}_{1/2}(\hat{\mathbf{k}}')]^{[0]}]\ . \tag{A6}$$

The completeness proof is finished once it is shown that

$$\int_0^\infty\kappa^2 d\kappa[\Delta_\ell^{J(-)}(k,\kappa)\Delta_\ell^{J(-)*}(k',\kappa)]=\frac{\delta(k-k')}{k^2}\ , \tag{A7}$$

and use is made of Eq. (A3) in Eq. (A6). Equation (A7) follows from the unitarity of the scattering amplitudes,

$$\mathrm{Im}f_\ell^{J(-)}(\kappa)=-\kappa\,|f_\ell^{J(-)}(\kappa)|^2\ , \tag{A8}$$

and the fact that they satisfy dispersion relations:

$$\frac{2}{\pi}\mathrm{P}\int_0^\infty\frac{k^2dk\,|f_\ell^{J(-)}(k)|^2}{[h_\ell^J(k)]^2(k^2-\kappa^2)}=\frac{\mathrm{Re}f_\ell^{J(-)}(\kappa)}{[h_\ell^J(\kappa)]^2}\ . \tag{A9}$$

As a consequence, all the terms that contain the scattering amplitude under the integral in Eq. (A6) cancel. All that remains is the pure delta-function term which leads to the right-hand side of Eq. (A7).

*Present address: Code 4651, Naval Research Laboratory, Washington, D.C. 20375.

[1]D. R. Lehman and M. Rajan, Phys. Rev. C **25**, 2743 (1982); W. C. Parke and D. R. Lehman, *ibid.* **29**, 2319 (1984).

[2]R. Ent, H. P. Blok, J. F. A. van Hienen, G. van der Steenhoven, J. F. J. van den Brand, J. W. A. den Herder, E. Jans, P. H. M. Keizer, L. Lapikas, E. N. M. Quint, P. K. A. de Witt Huberts, B. L. Berman, W. J. Briscoe, C. T. Christou, D. R. Lehman, B. E. Norum, and A. Saha, Phys. Rev. Lett. **57**, 2367 (1986).

[3]H. P. Blok, private communication.

[4]References can be found in C. T. Christou, Ph.D. dissertation, The George Washington University, 1986 (unpublished).

[5]D. R. Lehman, M. Rai, and A. Ghovanlou, Phys. Rev. C **17**, 744 (1978); A. Ghovanlou and D. R. Lehman, *ibid.* **9**, 1730 (1974).

[6]M. Rai, D. R. Lehman, and A. Ghovanlou, Phys. Lett. **59B**, 327 (1975).

[7]D. R. Lehman, Phys. Rev. **25**, 3146 (1982).

[8]D. R. Lehman and W. C. Parke, Few-Body Syst. **1**, 193 (1986).

[9]The integration methods/meshes are as follows: (1) infinite integration range–Gegenbauer/10 points, (2) angular integrals–Gaussian/6 points, and (3) κ (or E_κ) integral–variable-interval trapezoidal/563 points.

[10]Referring to the previous reference, the integration meshes for Tables I and II are 24, 24, and 563, respectively.

[11]This is clearly evident from Eq. (30) for the Y term, where the behavior of the $F_{\ell'(J\ell)}^{J'}(p)$ as $p\to 0$ is known from the integral equations. The X and Z terms require more manipulation to arrive at the same conclusion.

[12]S. Saito, J. Hiura, and H. Tanaka, Prog. Theor. Phys. **39**, 635 (1968).

[13]P. H. Wackman and N. Austern, Nucl. Phys. **30**, 529 (1962).